A Phenomenological Model of Photoinduced Surface Relief Formation in Arsenic Sulfide

Chao Lu, Daniel Recht, and Craig Arnold*
Princeton University
(Dated: January 9, 2013)

Chalcogenide materials, such as Arsenic Sulfide (As_2S_3), are well-known for their sensitivities to external stimuli, especially illumination. Among various photo-induced phenomena, this paper focused on mass transport issues. Thin films of As_2S_3 respond to non-uniform illumination by changing their surface morphologies. The volume expansion can be as large as 0.05% with appropriate illumination. However, there is still much debate on the mechanism for this process. We present a new model describing the surface structural modification by employing the incompressible fluid equation, driven by a photo-induced pressure. This equation, derived without any consumption of the microstructure of As_2S_3, is shown to be sufficient and effective in predicting many aspects of photo-induced surface relief formation.

PACS numbers: Valid PACS appear here

I. INTRODUCTION

It has long been known that photoinduced processes can lead to mass transport in a variety of systems generating surface relief. A variety of systems exhibit photoinduced expansion and or contraction.

While it has long been known that thin arsenic sulfide (As_2S_3) films expand when exposed to above-bandgap light, the mechanism by which this occurs is still open to debate [1–3]. Two fairly recent discoveries reveal that the situation is far more complex than it first appears. First, in 1994 Hisakuni and Tanaka found that exposure of As_2S_3 to laser light could induce expansions a full order of magnitude greater than had previously been observed even for very low intensities [4]. In order to explain this athermal effect, Hisakuni and Tanaka proposed and soon verified that As_2S_3 displays photoinduced fluidity [5].

The second major development was the discovery by Saliminia et al. (hereafter Saliminia) in 2000 that thin films of As_2S_3 will respond to the polarization of a Gaussian beam to which they are exposed by undergoing mass transport along the polarization vector [6]. Salminia's group also exposed films to several interference patterns with intensity gradients and to others with modulated polarization and observed the formation of surface relief gratings of a size comparable to the "giant" photoexpansion in both cases. Although surface relief gratings had been observed in the past, those early studies reported much smaller features [7]. In 2005, Asatryan et al. (hereafter Asatryan) repeated Saliminia's experiment at much lower intensities and found a similar result for polarization modulation but did not observe grating formation under intensity contrast [8]. Saliminia and Asatryan's results are summarized in table I.

After addressing and explaining the apparent contradictions between Saliminia and Asatryan's data, this paper presents a phenomenological model describing surface relief formation as incompressible flow driven by a photoinduced pressure and damped by surface tension. Despite the fact that both polarization and intensity modulation may lead to this effect, a single expression for the photoinduced pressure, derived without any assumptions about the microstructure of As_2S_3, is shown to be sufficient. Finally, results of the model are considered.

Illumination Conditions		**Surface Relief**	
Polarization of Initial Beams	**Modulated Quantity**	**Seen by Saliminia**	**Seen by Asatryan**
s-s	Intensity	$\frac{1}{2}$ p-p	None
p-p	Intensity	Major	None
s-p	Polarization	$\frac{3}{4}$ p-p	None
45-135	Polarization	$\approx$ p-p	Major
RCP-LCP	Polarization	Not tested	Major

TABLE I: A comparison of the observations reported by Saliminia and Asatryan concerning which illumination conditions lead to the formation of surface relief gratings. See figure 1 for a definition of s and p polarization in terms of the film's natural coordinate system. The angles in 45-135 polarization are measured above the positive x (s) axis. LCP and RCP refer respectively to left and right circular polarization.

II. THE MODEL

A. Reconciling Saliminia and Asatryan

The most important issue raised by table I is that Saliminia observed grating formation in response to intensity modulation while Asatryan did not. Naturally, one must look to their procedures for an answer. The most striking difference between their two studies is the intensity of the light used to illuminate the As_2S_3 films. While Saliminia used an intensity of 105 W/cm^2, Asatryan used just 350 mW/cm^2. One might be tempted to suggest

*Electronic address: cbarnold@princeton.edu

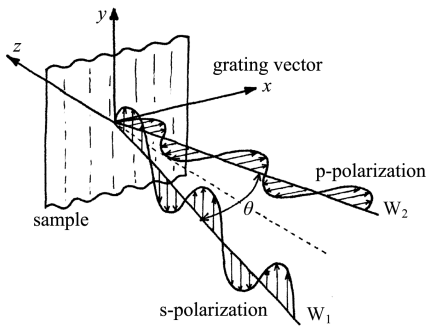

FIG. 1: Schematic diagram of the experimental setup used by Saliminia and Asatryan. Two beams, W1 and W2, interfere on the surface of a thin film of As_2S_3 leading to the pictured definitions of the coordinate system and polarization directions.

that 1) photoinduced fluidity is a necessary precursor to mass transport and 2) Asatryan's intensity was insufficient to bring this about. Unfortunately for this explanation, Trunov has shown conclusively that the intensity used by Asatryan would be more than enough to induce fluidity in As_2S_3 [9].

A close reading of Asatryan and Saliminia reveals another important, though easily overlooked discrepancy between their methods. In preparing films, Asatryan chose to expose them to a large fluence of circularly polarized light before testing for surface relief formation. As justification for this, she cites Lyubin's classic study of scalar and vector photoinduced phenomena in arsenic chalcogenides. While this paper does indeed report that scalar-vector pairs such as photoinduced changes in refractive index (a scalar effect) and photoinduced birefringence (its vector analogue) appear to operate according to different mechanisms, it does not imply that those mechanisms are completely independent as Asatryan seems to assume [10]. Nor can one take for granted, as Asatryan does by citing Lyubin, that all scalar and vector effects are due to the same underlying cause. These assumptions manifest themselves in Asatryan's neglect of the possibility, not addressed by Lyubin, that anisotropic activation of a scalar mechanism can produce vector results. This seems to be precisely the case observed by Saliminia. Specifically, Asatryan's saturation procedure corresponds to a larger scale version of Saliminia's exposure of a film to a circularly polarized Gaussian beam, a process that caused surface relief. Thus, Asatryan's pre-exposure could easily have saturated the intensity effect observed by Saliminia. It is therefore no wonder that Asatryan did not observe surface relief due to intensity modulation. However, the fact that Asatryan did manage to observe grating formation due to polarization modulation despite this saturation supports the existence of independent scalar and vector mass transport effects. In short, contrary to Asatryan's own assertions, there is no conflict between her results, Saliminia's study, and Lyubin's principles. In terms of the model being constructed, this discussion suggests that any expressions for the pressure will need to contain two independent components: one due to the vector effect and one due to its scalar counterpart.

B. Fluid Dynamics of Surface Relief Formation

Stipulating laminar flow of the glass and time-independent illumination that varies in one direction along the surface (the x axis) but is uniform along the other surface axis (y) and with depth (z) brings surface relief formation in As_2S_3 within the scope of the Navier-Stokes equation simplified into a two-dimensional boundary layer equation in x and z [11]. The coordinate system thus described is shown in figure 1.

$$\frac{\partial v_x}{\partial t} + v_x\frac{\partial v_x}{\partial x} + v_z\frac{\partial v_x}{\partial z} = -\frac{1}{\rho}\frac{\partial \mathcal{P}}{\partial x} + \nu\frac{\partial^2 v_x}{\partial z^2} + f, \quad (1)$$

in which the v_i's are components of the velocity vector, ρ is the mass density, $\mathcal{P}$ is the total pressure, f is the body force, and ν is the kinematic viscosity. approximation sanctions the replacement of $\mathcal{P}$ with its value at the surface since there is very little depth over which the pressure can change. At the surface, $\mathcal{P}$ comprises surface tension, $\mathcal{S}$, and the photoinduced pressure, P. Surface tension is traditionally taken to be proportional to surface curvature. Symbolically

$$\mathcal{S} = \sigma\frac{\frac{d^2h}{dx^2}}{\left[1+\left(\frac{dh}{dx}\right)^2\right]^{3/2}} \approx \sigma\frac{d^2h}{dx^2}, \quad (2)$$

where σ is a constant with units of force per length, h is the (spatially varying) thickness of the film, and the last step is justified by the thin film approximation since this condition implies $dh/dx \ll 1$. The photoinduced pressure, which is simply assumed to exist, is discussed at length in Section II C. For now it is enough to note that since the illumination is modulated only along the x axis, the photoinduced pressure can vary only with x. The thin film approximation thus makes it possible to say that

$$\mathcal{P} \approx P(x) - \sigma\frac{\partial^2 h}{\partial x^2}. \quad (3)$$

In addition, there are no body forces to speak of so $f = 0$.

Combining this information with equation 1 leads to

$$\frac{\partial v_x}{\partial t} + v_x\frac{\partial v_x}{\partial x} + v_z\frac{\partial v_x}{\partial z} = -\frac{1}{\rho}\frac{\partial}{\partial x}\left[P(x) - \sigma\frac{\partial^2 h}{\partial x^2}\right] + \nu\frac{\partial^2 v_x}{\partial z^2}. \quad (4)$$

The thin film approximation also implies that

$$v_x \frac{\partial v_x}{\partial x} \ll v_z \frac{\partial v_x}{\partial z} \tag{5}$$

since v_x and v_z are of roughly the same order and the film is assumed to be much wider than it is thick. That accounts for one term in equation 4, but more can be said. Following the analyses of Ledoyen et al. and Pimputkar et al., it is possible to drop all the terms on the right-hand side because they turn out to be small in practice [12–14]. Doing so yields

$$\frac{\partial^2 v_x}{\partial z^2} \approx \frac{1}{\eta}\left[\frac{\partial P(x)}{\partial x} - \sigma \frac{\partial^3 h}{\partial x^3}\right], \tag{6}$$

where $\eta = \rho\nu$ is the dynamic viscosity.

Equation 6 appears to be solvable. Hence, it is time to compile a list of constraints and boundary conditions. The first of these is the continuity equation

$$\frac{\partial v_x}{\partial x} + \frac{\partial v_z}{\partial z} = 0, \tag{7}$$

which is derived from incompressibility and conservation of mass. Next, assuming perfect adhesion to the substrate implies

$$v_x = v_z = 0 \text{ at } z = 0, \tag{8}$$

where $z = 0$ is the film-substrate interface. At the free surface of the film, the shear stress along z goes to zero [11, 14]. Symbolically,

$$\frac{\partial v_x}{\partial z} = 0 \text{ at } z = h. \tag{9}$$

Finally, the z velocity at the free surface is the rate of change in the height. This can be represented formally as

$$v_z = \frac{\partial h}{\partial t} \text{ at } z = h. \tag{10}$$

As will become evident, equations 7 through 10 are enough to specify the problem.

Since the right-hand side of equation 6 has no z dependence, the whole equation can be integrated with respect to z.

$$\frac{\partial v_x}{\partial z} \approx \frac{z}{\eta}\left[\frac{\partial P(x)}{\partial x} - \sigma \frac{\partial^3 h}{\partial x^3}\right] + C_1, \tag{11}$$

where C_1 is an integration constant. Applying the shear stress boundary condition (equation 9) allows for the determination of C_1. Thus

$$\frac{\partial v_x}{\partial z} \approx \frac{(z-h)}{\eta}\left[\frac{\partial P(x)}{\partial x} - \sigma \frac{\partial^3 h}{\partial x^3}\right]. \tag{12}$$

Integrating with respect to z again gives

$$v_x \approx \frac{\left(z^2/2 - hz\right)}{\eta}\left[\frac{\partial P(x)}{\partial x} - \sigma \frac{\partial^3 h}{\partial x^3}\right] + C_2. \tag{13}$$

Application of the x part of the substrate boundary condition (equation 8) clearly shows that C_2 is 0. Taking the derivative of both sides with respect to x and applying the continuity condition (equation 7) yields

$$-\frac{\partial v_z}{\partial z} \approx \frac{\partial}{\partial x}\left(\frac{\left(z^2/2 - hz\right)}{\eta}\left[\frac{\partial P(x)}{\partial x} - \sigma \frac{\partial^3 h}{\partial x^3}\right]\right). \tag{14}$$

This too can be integrated with respect to z.

$$-v_z \approx \frac{\partial}{\partial x}\left(\frac{\left(z^3/6 - hz^2/2\right)}{\eta}\left[\frac{\partial P(x)}{\partial x} - \sigma \frac{\partial^3 h}{\partial x^3}\right]\right) + C_3 \tag{15}$$

The z part of the substrate boundary condition reveals C_3 to be 0 as well.

Finally, setting $z = h$ and applying the last boundary condition (equation 10) gives

$$\frac{\partial h}{\partial t} \approx \frac{\partial}{\partial x}\left(\frac{h^3}{3\eta}\left[\frac{\partial P(x)}{\partial x} - \sigma \frac{\partial^3 h}{\partial x^3}\right]\right). \tag{16}$$

Given $P(x)$, equation 16 is readily solvable by standard numerical methods. Accordingly, the final component of this model is a suitable expression for this function. Before accepting it and moving on, however, prudence recommends the application of some physical intuition. Equation 16 gives the spatial dependence of the rate and direction of surface relief formation. It seems reasonable that this rate be inversely proportional to the viscosity of the film. Furthermore, noting that the pressure is some function of the electric field, the appearance of its gradient (which must depend, at least in part, on the electric field gradient) is reminiscent of Saliminia's rough model discussed in Section II A [6]. Naively speaking, this means that shortening the period of electric field variation should increase the magnitude of the surface relief growth rate. This effect is then countered by the corresponding increase in the surface tension since shorter periods have more curvature. All in all, the picture of balance thus painted is quite believable.

C. Quantifying the Pressure

In general, the photoinduced pressure can depend anisotropically on the electric field of the incident light. Symbolically, $P = P(E_x, E_y)$. This function can be expanded in the complex components E_x and E_y (see figure 1) according to

$$P(E_x, E_y) = a_1 E_x + a_2 E_y + a_3 E_x^2 + a_4 E_x E_y + a_5 E_y^2 + \mathcal{O}(3), \tag{17}$$

where the a_i's are real constants. Absent from equation 17 is a provision to ensure that the pressure is real. Two choices can be thrown away immediately: taking the real part of the entire right-hand side of equation 17 and saying that $P(E_x, E_y) = P(|E_x|, |E_y|)$. The former leads to pressures that oscillate rapidly in time about a mean

of 0. The latter ignores all phase information and thus cannot hope to explain s-p interference.

The appropriate choice is to require that $P(E_x, E_y) = P(\tilde{E}_x, \tilde{E}_y)$ where $\tilde{E}_x = \Re\mathrm{e}\{E_x\}$ [15]. In this case, 17 becomes

$$P(E_x, E_y) = a_1\tilde{E}_x + a_2\tilde{E}_y + a_3\tilde{E}_x{}^2 + a_4\tilde{E}_x\tilde{E}_y + a_5\tilde{E}_y{}^2 + \mathcal{O}(3). \tag{18}$$

Now, the electric field oscillates so quickly that one could not reasonably expect the As_2S_3 to respond to it in other than a time-averaged manner. Since the time averages of $\tilde{E}_x$ and $\tilde{E}_y$ are both 0, they can be dropped from equation 18. Thus, ignoring third and higher order terms

$$P(E_x, E_y) \approx \left\langle a_3\tilde{E}_x{}^2 + a_4\tilde{E}_x\tilde{E}_y + a_5\tilde{E}_y{}^2 \right\rangle, \tag{19}$$

where angular brackets indicate time averaging.

Further consideration of the pressure arises from its physical origin (see figure 2 and 3). The diffusion units, which are size of medium order range (up to 2 coordination sphere), are simplified to be the electrical-induced dipoles. The strength of the dipoles could be calculated by equation $\vec{P} = \int d^3r\rho(\vec{r})\vec{r}$, where the charge distribution $\rho(\vec{r})$ could be obtained from quantum calculation with high accuracy. At the present of optical radiation, the weak connections in-between the diffusion units, which is the van der waals force, are broken, then these units are free to move, so our treatment using Navier-Stokes equations to describe the diffusion process is appropriate. Furthermore, the electrical field of the light modify the diffusion units to be induced dipoles. Those dipoles starts to align and move according to the polarization of electrical field, until the balance is achieved, where new connection, i.e. van der waals interactions are built up again. It is by this way, the units diffuses, leading to the surface morphology modified by the optical field.

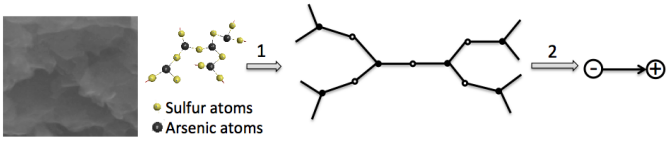

FIG. 2: The diffusion units are assumed to be optical-induced dipoles. The figure on the left is a SEM observation of the layered structure of As_2S_3; those layers are diffusion units.

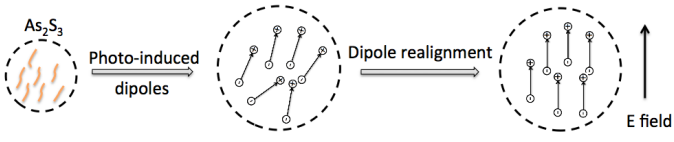

FIG. 3: Dipole realignment under electrical field causes diffusion, leading to the volume expansion.

Now we are able to calculate the photo-induced pressure theoretically. Since pressure is always proportional to energy density so we start with relation $Pressure \propto \partial Energy/\partial V$. Equations describing the total free energy density of such dipole interaction system in present of the electric field are present in Landau's textbook [16],

$$Energy = F_0 + \epsilon_{ik}\epsilon_0 E_i E_k. \tag{20}$$

Where F_0 is the free energy of the system in absence of an external field. In the dipole interaction model, ϵ_{ik} actually describes the polarizability of diffusion units when exposed to electric field of the light. Rigorous result for the pressure is obtained from equation 20, in terms of the stress tensor, which is taken from the Landau's textbook [16],

$$\sigma_{ik} = \epsilon_0 E_i D_k. \tag{21}$$

Plugging $D_k = \Sigma(\epsilon_{km}E_m)$ into equation 21, the stress tensor is simplified as

$$\sigma_{ik} = \epsilon_0 E_i(\epsilon_{kx}E_x + \epsilon_{ky}E_y + \epsilon_{kz}E_z). \tag{22}$$

Taking trace of the stress tensor then applying the time average, the pressure is written as

$$\begin{aligned} P &= \frac{1}{3}\langle Trace(\sigma)\rangle \\ &= \frac{1}{3}\langle \sigma_{xx} + \sigma_{yy} + \sigma_{zz}\rangle \\ &= \frac{\epsilon_0}{3}\langle E_x(\epsilon_{xx}E_x + \epsilon_{xy}E_y) + E_y(\epsilon_{yx}E_x + \epsilon_{yy}E_y)\rangle \\ &= \frac{\epsilon_0}{3}\langle \epsilon_{xx}E_x^2 + 2\epsilon_{xy}E_xE_y + \epsilon_{yy}E_y^2\rangle. \end{aligned} \tag{23}$$

Again, to ensure the pressure is real, equation of the pressure is further derived as

$$\begin{aligned} P(E_x, E_y) &= P(\tilde{E}_x, \tilde{E}_y) \\ &= \frac{\epsilon_0}{3}\langle \epsilon_{xx}\tilde{E}_x{}^2 + 2\epsilon_{xy}\tilde{E}_x\tilde{E}_y + \epsilon_{yy}\tilde{E}_y{}^2\rangle. \end{aligned} \tag{24}$$

Comparing equations 19 and 24, one can easily figure out the coefficients in 19 actually have their physical correspondence, i.e., the polarizablity of the material, which could be measured experimentally. With these coefficients, the optical induced pressure is readily calculated.

D. Simulation

In the holographic setups used by Saliminia and Asatryan, everything about the two interfering beams was identical except for their polarizations and the direction of their wave vectors. The most general electric field produced by such interference can be written

$$e^{i(kx-\omega t)}\begin{pmatrix} |E_x|\, e^{i\phi_x} \\ |E_y|\, e^{i\phi_y} \end{pmatrix}, \tag{25}$$

Polarization	$I(x)$	$\psi(x)$	$\Delta\phi(x)$	$P(x)$
s-s	$2E_0^2\,(1+\cos 2\delta)$	$\pi/2$	0	$(c_1-c_2)2E_0^2\,(1+\cos 2\delta)$
p-p	$2E_0^2\,(1+\cos 2\delta)$	0	0	$(c_1+c_2)2E_0^2\,(1+\cos 2\delta)$
s-p	$2E_0^2$	$\pi/4$	-2δ	$2E_0^2\,(c_1+c_3\cos 2\delta)$
45-135	$2E_0^2$	δ	$-\pi/2$	$2E_0^2\,(c_1+c_2\cos 2\delta)$
LCP-RCP	$2E_0^2$	δ	0	$2E_0^2\,(c_1+c_2\cos 2\delta+c_3\sin 2\delta)$
				$=2E_0^2\left(c_1+\sqrt{c_2^2+c_3^2}\sin\left[2\delta+\arctan\left(c_3/c_2\right)\right]\right)$

TABLE II: Summary of the photoinduced pressure predicted by equation 28 for various polarization conditions. I, ψ, and $\Delta\phi$ can easily be derived from the interference of plane waves. $\delta=\frac{2\pi}{\lambda}x\sin\frac{\theta}{2}$ for θ as in figure 1. A trigonometric identity was used to derive the second form of $P(x)$ for LCP-RCP interference in order to show that for all cases considered $P(x)$ can be expressed as twice the intensity of one of the initial beams times the sum of a constant and a sinusoidal oscillation.

where $|E_x|$, $|E_y|$, ϕ_x, and ϕ_y are arbitrary, real, and time (but not necessarily position) independent. Taking E_x and E_y from 25, plugging them into 24, and computing the time averages gives

$$P\approx b_1\left|E_x\right|^2+b_2\left|E_y\right|^2+b_3\left|E_x\right|\left|E_y\right|\cos\Delta\phi, \qquad (26)$$

where $b_1=\epsilon_0\epsilon_{xx}/6$, $b_2=\epsilon_0\epsilon_{yy}/6$ and $b_3=\epsilon_0\epsilon_{xy}/3$. Defining a generalized polarization angle (applicable to elliptical polarizations) $\psi=\arctan\left|E_y\right|/\left|E_x\right|$, equation 26 can be rewritten as

$$\begin{aligned} P &\approx I\left[b_1\cos^2\psi+b_2\sin^2\psi+b_3\sin 2\psi\cos\Delta\phi\right] && (27)\\ &= I(x)\left[c_1+c_2\cos 2\psi(x)+c_3\cos\Delta\phi(x)\sin 2\psi(x)\right], && (28)\end{aligned}$$

where the x dependence explicitly indicated in going from equation 27 to equation 28, while the coefficients have been redefined and calculated as: $c_1=\epsilon_0\epsilon_{xx}/6$, $c_2=\epsilon_0(\epsilon_{yy}-\epsilon_{xx})/6$ and $c_3=\epsilon_0\epsilon_{xy}/3$. Equation 28 seems intuitively reasonable since it depends on intensity, polarization, and $\Delta\phi$, the three quantities modulation of which can cause surface relief. Taking the first spatial derivative of Equation 28 yields

$$\begin{aligned}\frac{\partial P}{\partial x} &\approx \frac{\partial I}{\partial x}\left[c_1+c_2\cos 2\psi(x)+c_3\cos\Delta\phi(x)\sin 2\psi(x)\right]\\ &\quad+2I(x)\frac{\partial\psi}{\partial x}\left[-c_2\sin 2\psi(x)+c_3\cos\Delta\phi(x)\cos 2\psi(x)\right]\\ &\quad+I(x)\frac{\partial\Delta\phi}{\partial x}\left[-c_3\sin\Delta\phi(x)\sin 2\psi(x)\right]. \qquad (29)\end{aligned}$$

Equation 29 cleanly separates into three independent terms governing the pressure gradient induced by modulation of intensity, polarization direction, and phase. Accordingly, this model is consistent with the idea suggested by the data that the intensity and phase modulation terms arise from the scalar effect while the angle modulation term is due to the vector phenomenon. Further study is required to determine the exact mechanism by which this occurs, though two possibilities can be identified at this point. One is that certain bonds are excited by intensity and phase modulation and others by polarization modulation; another is that the different illumination conditions drive different electronic transitions in the material's band structure. That said, this phenomenon could be due to an effect that is entirely different from those considered above. Fortunately, the present discussion suggests that the phenomenological approach embodied by equation 29 could serve as the skeleton for a complete physical model no matter what the fundamental mechanism turns out to be.

Table II lists the pressure functions predicted by equation 28 for each of the polarization conditions tested by Saliminia and Asatryan. Despite the widely varying initial conditions considered, the $P(x)$'s are all of roughly the same form. Interestingly, the c_i's enter in a way that evokes Saliminia's observations of the dependence of grating amplitude's on the polarizations of the interfering beams (see table I). Specifically, setting $c_2=3c_1$ and $c_3=2c_1$ begins to approximate Saliminia's qualitative description of the observed size ordering. [17]

Recalling that E_0^2 has a Gaussian profile (coming, as it does, from a laser), it is fair to model the pressure as

$$P\sim p_1e^{-2(x/p_2)^2}\left[p_3+\cos\left(p_4x+p_5\right)\right] \qquad (30)$$

where the p_i's are, roughly speaking, fitting parameters (with p_5 included to account for the possibility that the Gaussian intensity profile is not centered on a peak of the modulation). In practice, the experimental setup fixes p_2 (the modulation frequency) and p_4 (the beam radius) which are the same across all polarization conditions. On the other hand, p_1, p_3, and to a lesser extent p_5 are true degrees of freedom which can be used to fit the model to observations.

III. RESULTS

While equations 16 and 30 and the requirements of the numerical methods used specify nine constants of interest, most are set by the experimental procedure or the equations in table II. The model parameters, both fixed and free, are summarized in table IV. Of particular note are p_1, η, and σ. Rewriting the pressure as $p_1\hat{P}(x)$ allows

Parameter	Meaning	Value
	Fixed Parameters	
h_0	Initial Thickness	2 μm
T	Total Illumination Time	381 s
p_2	Illumination Radius	57 μm
p_3	Non-Oscillatory Pressure	1
p_4	Modulation Frequency	$2\pi/13$ μm^{-1}
p_5	Modulation Phase	$\pi/2$
	Free Parameters	
p_1/σ	Relative Pressure Strength	0.88 μm^{-1}
σ/η	Characteristic Growth Rate	1.9×10^{-3} μm/s

TABLE III: Summary of the parameters used in constructing the fit depicted in figure 4.

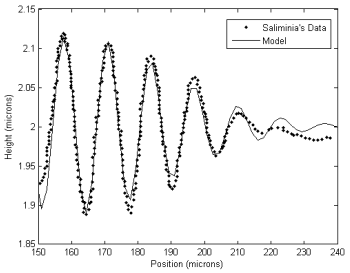

FIG. 4: The model's fit to a section of a surface relief profile from Saliminia's paper.

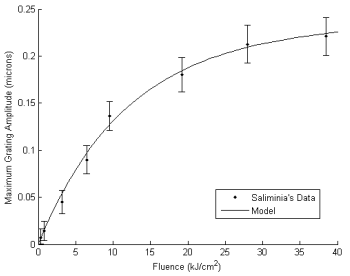

FIG. 5: Fluence (time) dependence of maximum surface relief amplitude for the fit in figure 4. The x axis corrects an apparent typographical error in Saliminia's original paper.

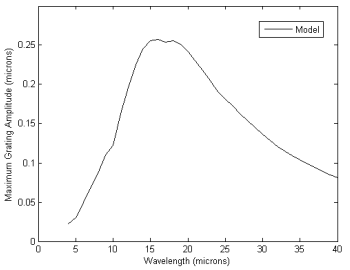

FIG. 6: Dependence of the predicted maximum surface relief amplitude on spatial modulation frequency with all other parameters as in table IV. Although inconsistencies in Saliminia's reporting prevent a fit, the curve presented matches all the major qualitative features of Saliminia's graph.

for the recasting of equation 16 as

$$\frac{\partial h}{\partial t} \approx \frac{\partial}{\partial x}\left(\frac{\sigma h^3}{3\eta}\left[\frac{p_1}{\sigma}\frac{\partial \hat{P}(x)}{\partial x} - \frac{\partial^3 h}{\partial x^3}\right]\right) \tag{31}$$

which reduces the number of constants to eight and the number of fitting parameters to two, σ/η (a material property) and p_1/σ (the relative pressure strength). figure 4 shows the model's fit to a section of a surface relief profile from Saliminia's paper. The parameter values used in producing this fit are shown in table IV. As can be seen from figure 5, the fit thus produced also displays the correct time dependence. Finally, figure 6 reveals that the model can account for the observed dependence of grating amplitude on modulation period.

Parameter	Meaning	Value
	Fixed Parameters	
h_0	Initial Thickness	2 μm
T	Total Illumination Time	381 s
p_2	Illumination Radius	57 μm
p_3	Non-Oscillatory Pressure	1
p_4	Modulation Frequency	$2\pi/13$ μm^{-1}
p_5	Modulation Phase	$\pi/2$
	Free Parameters	
p_1/σ	Relative Pressure Strength	0.88 μm^{-1}
σ/η	Characteristic Growth Rate	1.9×10^{-3} μm/s

TABLE IV: Summary of the parameters used in constructing the fit depicted in figure 4.

[1] T. Igo, Y. Noguchi, and H. Nagai, Applied Physics Letters **25**, 193 (1974).

[2] J. Hegedus, K. Kohary, and S. Kugler, Jounral of Optoelectronics and Advanced Materials **7**, 2231 (2005).

[3] A. Ganjoo, K. Shimakawa, K. Kitano, and E. A. Davis, Journal of Non-Crystalline Solids pp. 917–923 (2002).

[4] H. Hisakuni and K. Tanaka, Applied Physics Letters **65**, 2925 (1994).

[5] H. Hisakuni and K. Tanaka, Science **270**, 974 (1995).

[6] A. Saliminia, T. V. Galstian, and A. Villeneuve, Physical Review Letters **85**, 4112 (2000).

[7] T. V. Galstyan, J. F. Viens, A. Villeneuve, K. Richardson, and M. A. Duguay, Journal of Lightwave Technology **15**, 1343 (1997), 0733-8724.

[8] K. E. Asatryan, T. Galstian, and R. Vallée, Physical Review Letters **94**, 087401 (2005).

[9] M. L. Trunov and V. S. Bilanich, Journal of Optoelectronics and Advanced Materials **5**, 1085 (2003).

[10] V. M. Lyubin and V. K. Tikhomirov, Journal of Non-Crystalline Solids **114**, 133 (1989).

[11] V. Levich, *Physiochemical Hydrodynamics* (Prentice-Hall, Englewood Cliffs, NJ, 1962), 2nd ed., pp. 372-376 and 669-671.

[12] F. Ledoyen, P. Bouchard, D. Hennequin, and M. Cormier, Physical Review A **41**, 4895 (1990).

[13] S. Pimputkar and S. Ostrach, Physics of Fluids **23**, 1281 (1980), URL `http://link.aip.org/link/?PFL/23/1281/1`.

[14] C. J. Barrett, P. L. Rochon, and A. L. Natansohn, Journal of Chemical Physics **109**, 1505 (1998).

[15] D. L. Recht, *A phenomenological model of photoinduced surface relief formation in arsenic sulfide* (2006), Princeton University Thesis.

[16] L. D. Landau and E. M. Lifshitz, *Electrodynamics of Continuous Media* (Pergamon Press LTD., 1960), pp. 58-69.

[17] It does not matter that this scheme makes $P(x)$ negative for s-s interference since this serves only to change the phase of the spatial oscillations in the magnitude of of $\partial P(x)/\partial x$